END

FILMED

DTIC

CRREL

REPORT 85-3

AD-154 046
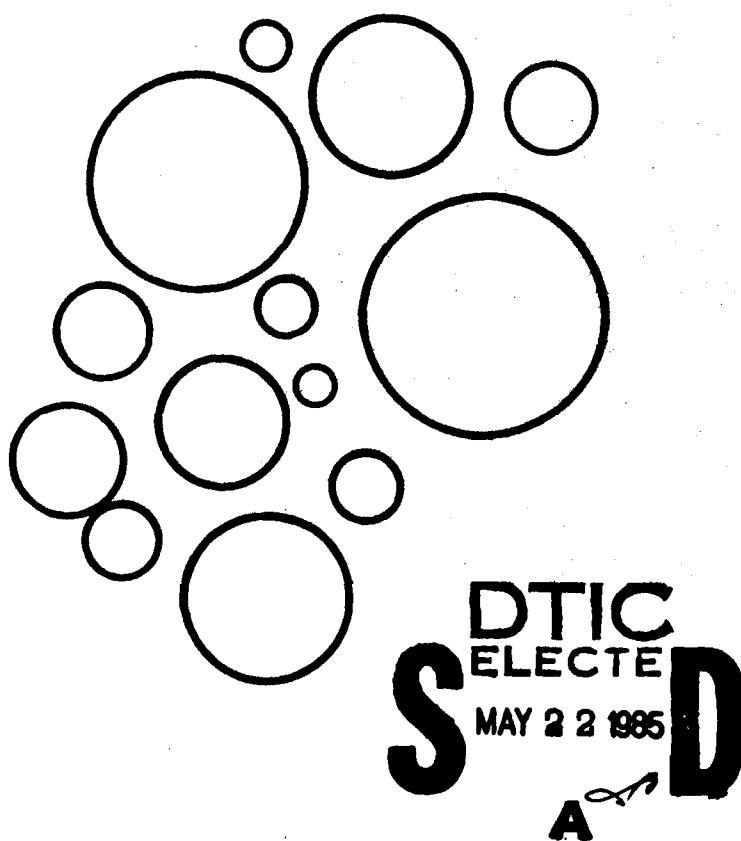
**US Army Corps
of Engineers**

Cold Regions Research &
Engineering Laboratory

*Effect of nonuniform size on internal
stresses in a rapid, simple shear flow of
granular materials*

Part 2. Multiple grain sizes

X_2

$u(X_2)$

X_1

85 04 24 075

For conversion of SI metric units to U.S./British customary units of measurement consult ASTM Standard E380, Metric Practice Guide, *published by the American Society for Testing and Materials, 1916 Race St., Philadelphia, Pa. 19103.*

Cover: Shear flow of multiple sizes of spheres.

Effect of nonuniform size on internal stresses in a rapid, simple shear flow of granular materials

Part 2. Multiple grain sizes

Hayley H. Shen
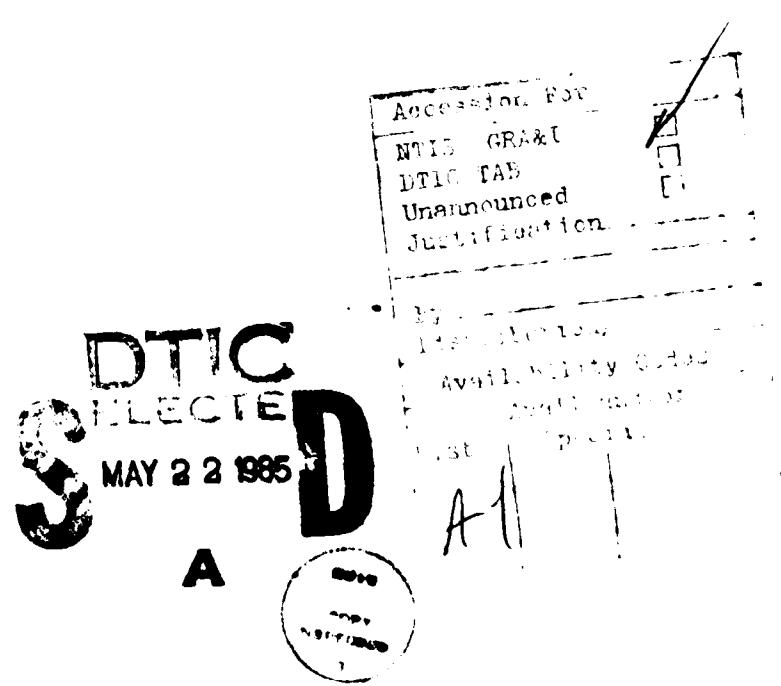
REPORT DOCUMENTATION PAGE		READ INSTRUCTIONS BEFORE COMPLETING FORM
1. REPORT NUMBER CRREL Report 85-3	2. GOVT ACCESSION NO. AD-A154046	3. RECIPIENT'S CATALOG NUMBER
4. TITLE *(and Subtitle)* EFFECT OF NONUNIFORM SIZE ON INTERNAL STRESSES IN A RAPID, SIMPLE SHEAR FLOW OF GRANULAR MATERIALS: Part 2. Multiple Grain Sizes		5. TYPE OF REPORT & PERIOD COVERED
		6. PERFORMING ORG. REPORT NUMBER
7. AUTHOR(s) Hayley H. Shen		8. CONTRACT OR GRANT NUMBER(s)
9. PERFORMING ORGANIZATION NAME AND ADDRESS U.S. Army Cold Regions Research and Engineering Laboratory Hanover, New Hampshire 03755-1290		10. PROGRAM ELEMENT, PROJECT, TASK AREA & WORK UNIT NUMBERS
11. CONTROLLING OFFICE NAME AND ADDRESS U.S. Army Cold Regions Research and Engineering Laboratory Hanover, New Hampshire 03755-1290		12. REPORT DATE February 1985
		13. NUMBER OF PAGES 29
14. MONITORING AGENCY NAME & ADDRESS*(if different from Controlling Office)*		15. SECURITY CLASS. *(of this report)* Unclassified
		15a. DECLASSIFICATION/DOWNGRADING SCHEDULE

16. DISTRIBUTION STATEMENT *(of this Report)*

Approved for public release; distribution is unlimited.

17. DISTRIBUTION STATEMENT *(of the abstract entered in Block 20, if different from Report)*

18. SUPPLEMENTARY NOTES

19. KEY WORDS *(Continue on reverse side if necessary and identify by block number)*

Flow
Granular flow
Particle size distribution

20. ABSTRACT *(Continue on reverse side if necessary and identify by block number)*

In the past all theoretical analyses for rapidly sheared granular flows assumed that the granular solids are either disks or spheres and are uniform in size. However, natural materials that create these granular flows are in general irregular in shape and have various spectra of sizes. The stress and rate of energy dissipation levels in granular flows are significantly influenced by the size distribution. In part 1 of this report series, the formulation of the constitutive equations considering a two-size granular mixture is presented, where the ratio of the two sizes is nearly one. Here, in part 2, the constitutive equations for a two-size mixture are extended to include a general size ratio. In addition, a complete spectrum of size distribution is incorporated, which allows the quantification of the size distribution effect in the most general way. In analyzing the stresses, intergranular collision is assumed to be the major dynamic activity at the microscopic level.

20. Abstract (cont'd).

Because of the present limited knowledge of treating shape effects, the analysis is confined to the flow of either disks or spheres. The result of this work provides necessary information for a more realistic analysis of natural and industrial granular flows.

PREFACE

CONTENTS

ILLUSTRATIONS

NOMENCLATURE

A_L	πD_L^2
C	total volume concentration
C_D	probability density function of volume concentration
C_L, C_S	partial volume concentrations
C_{Lo}, C_{So}	densest partial volume concentrations
C_o	densest random volume concentration
C_{Sa}	actual volume concentration of small spheres
D, D'	diameters
D_L, D_S	diameters of large and small spheres
D_M	mean diameter
d	thickness of a disk
$\overline{E}$	average energy dissipation in a pair of identical spheres
$\overline{E}_{DD'}, \overline{E}_{LL}, \overline{E}_{LS}, \overline{E}_{SS}$	average energy dissipation in a pair of like or unlike spheres
f	collision frequency/2
$F(D)$	probability distribution
G_D, G_L, G_S	number densities
L, S	large and small
ℓ	distance traveled before a collision
$\Delta \overline{M}_{DD'1}, \Delta \overline{M}_{DD'2},$ $\Delta \overline{M}_{LL1}, \Delta \overline{M}_{LL2},$ $\Delta \overline{M}_{LS1}, \Delta \overline{M}_{LS2},$ $\Delta \overline{M}_{SL1}, \Delta \overline{M}_{SL2},$ $\Delta \overline{M}_{SS1}, \Delta \overline{M}_{SS2}$	average momentum transfer between like or unlike spheres in the x_1, x_2 directions
$\Delta \overline{M}_j$	average momentum transfer in the x_j direction
$\Delta \overline{M}_{PQ_j}$	average momentum transfer between a P-size and a Q-size sphere in the x_j direction
N_D	number of spheres with diameter D in a unit volume
N_L, N_S	number of large or small spheres in a unit volume
N_{LL}, N_{LS}, N_{SS}	collision frequencies between like or unlike spheres in a unit volume
$N_{DD'}^s, N_{LL}^s, N_{LS}^s, N_{SL}^s$	collision frequencies for a specific sphere
N_{PQ}^s	collision frequency between a P-size sphere and all the neighboring Q-size spheres
P, Q	indices for sphere size
$P(D)$	probability density function
p_D	number density of spheres with diameter D on a unit surface
p_i	number density of spheres on a unit surface normal to x_i direction
$p_{L1}, p_{L2}, p_{S1}, p_{S2}$	number densities of large or small spheres on a unit surface normal to x_1 or x_2 direction
p_{Pi}	number density of P-size spheres on a unit surface normal to x_i direction
p_S	number density of small spheres on a unit surface
R	average radius of a cell
R_L, R_S	average radii of cells centered at large or small spheres
RC	C_S/C_L
RD	D_S/D_L
s	average gap between adjacent spheres
s_L, s_S	average gap between adjacent large or small spheres
u	mean velocity
$\overline{V}_L$	average relative velocity of large spheres
$v_D', v_{D'}', v_L', v_S'$	fluctuation velocities
v_{DM}'	fluctuation velocity of mean size spheres
x_1, x_2	coordinates

α, ϕ, θ	angles
ϵ	restitution coefficient
η, σ	parameters for log-normal distribution
μ	coefficient of friction
ρ_s	solid density
$\bar{\tau}$	nondimensional shear stress
τ_{ij}	stress in the x_j direction on a plane normal to x_i direction
τ_{21}, τ_{22}	shear and normal stresses on a plane normal to x_2 direction

EFFECT OF NONUNIFORM SIZE ON INTERNAL STRESSES IN A RAPID, SIMPLE SHEAR FLOW OF GRANULAR MATERIALS
Part 2. Multiple Grain Sizes

Hayley H. Shen

INTRODUCTION

The flow of a granular material is a dynamic phenomenon that can be modeled by macroscopic equations describing the balance of mass, momentum and energy within the system. A correct formulation of the stresses and the rate of energy input–output is crucial to the success of a mathematical model of such a system. The mathematical formulations of the stresses and the rate of energy input–output are called the constitutive equations. The constitutive equations for a flowing granular material can range over a wide spectrum, from Newtonian to highly non-Newtonian forms.

Although a nondimensional parameter that determines the form of the constitutive relations is unknown yet, it is believed that the flow rate, the concentration and the material properties of the granular solids determine the regime of the granular flow and hence the form of the constitutive equations.

Within a given flow regime, the constitutive relations are determined by the way energy and momentum are transferred microscopically from one location to another. Different transferring mechanisms produce different constitutive equations. Two examples of such different constitutive equations can be found in Bagnold (1954) where either a linear or a quadratic stress–strain-rate relation is used, depending on the flow regime. In slow flow viscous dissipation in the granular interstice dominates and gives a linear stress–strain-rate relation, while in a fast flow, dissipation by collisions among granules dominates and gives a quadratic stress–strain-rate relation similar to those in a turbulent fluid flow. Another type of constitutive relation has been derived for deforming ice fields in the polar seas where pressure ridge formation was the major dynamic activity (e.g. Rothrock 1975). It is found that the stress-strain-rate relation is of the plastic type. Recently, however, there have been some doubts about the applicability of this constitutive law to the ice edge where concentration is too low to form ridges.

In the past few years, a number of researchers have formulated constitutive equations for granular flows (Kanatani 1979, Ogawa et al. 1980, Shen and Ackermann 1982, Campbell and Brennen 1983, Walton 1983, Jenkins and Savage 1983 and Lun et al. 1984), and most of these have assumed intergranular collisions to be the major momentum transfer and energy dissipation mechanism. The resulting constitutive equations are quadratic and check well with experimental data (Shen and Ackermann 1982). The above researchers found that the stress level generated in such

a granular flow depends crucially on material properties of the physical constituents: the restitution and frictional coefficient, densities of the granular solid and the interstitial fluid, and the drag coefficient of the fluid.

While able to give a great deal of physical insight into the dynamics of a fast granular flow, the above studies assumed that the granular solids are either disks or spheres and are uniform in size. Natural materials of interest are generally irregular in shape and have various sizes. As evidenced by experiments on sediment transport (e.g. Gilbert 1914, Durand 1953), under the same driving mechanism, a widely graded sediment is transported at a much higher rate than a relatively uniformly graded sediment. These phenomena suggest that the stress levels and the rate of energy dissipation are significantly influenced by the size distribution existing in the flowing granular material.

This report presents the formulation of constitutive equations incorporating a size distribution in the granular material. Intergranular collision is assumed the major dynamic activity at the microscopic level, as in an earlier work where granular materials of one size were considered (Shen and Ackermann 1982). Because of the present limited knowledge of how to treat shape effects, the analysis will be confined to the flow of either disks or spheres. Nevertheless, the result of this work provides information necessary to a more realistic analysis of virtually any natural granular flow, including drifting ice fields in the polar seas and avalanches of snow or debris.

The analysis for a complete spectrum of sizes is based on the result of analyzing a two-size mixture (Shen 1985). For the sake of completeness, the analysis for a two-size mixture is reviewed briefly in what follows; the details are given in the companion to this report, *Effect of nonuniform size on internal stresses in a rapid, simple shear flow of granular materials: Part 1. Two grain sizes.*

The two-size mixture considered here is an assembly of spherical particles because spherical particles model a wide variety of natural materials and because the only existing experimental data for direct comparison with the theory were obtained for spherical particles. However, it is a straightforward extension to apply the same analysis to disks. The complete spectrum analysis will be carried out for both spheres and disks.

CONSTITUTIVE EQUATIONS FOR A TWO-SIZE MIXTURE

Assume a homogeneous mixture of spheres with two sizes under a simple shear motion as illustrated in Figure 1. The interstitial fluid effect is not included in this model. In a crude way, the interstitial fluid effect can be treated as did Ackermann and Shen (1982). The diameters of the large and small spheres are D_L and D_S respectively. Although extending this model to mixtures of different material properties is a straightforward matter, in the present study only the size effect is considered. The material property for all spheres is thus the same and includes the density ρ_s, the restitution coefficient ϵ, and the frictional coefficient μ.

Figure 1. Shear flow of a mixture of spheres.

Let G_L and G_S denote the number percentages of the large and small spheres in a unit volume respectively. This means that if $G_L : G_S = 70:30$, there are 70 large spheres and 30 small ones in a random sample of 100 spheres. The ratio of large to small spheres surrounding an average sphere is $G_L : G_S$. For a given combination of G_L, G_S and D_L, D_S, let C_o denote the volume concentration of the spheres when all neighboring spheres are touching, i.e., C_o is the volume concentration for the densest random packing. If all spheres are then separated by the distance s away from the neighboring ones, the volume concentration C for this looser state is

$$C = C_o [R/(R+s)]^3 \tag{1}$$

where R is the radius of a typical "cell" formed by a given sphere and all its neighboring spheres (the power becomes 2 for disk-shaped material), and is given as (Shen 1985):

$$R = G_L R_L + G_S R_S \tag{2}$$

where

$$R_L = G_L D_L + G_S (D_L + D_S)/2 \tag{3a}$$

$$R_S = G_L (D_L + D_S)/2 + G_S D_S . \tag{3b}$$

When sheared, the assembly of these spheres will start to collide with each other and produce velocity fluctuations. The momentum transfer caused by these collisions gives rise to stresses which are modeled as (Bagnold 1954):

$$\tau_{ij} = p_i \cdot f \cdot \Delta M_j \tag{4}$$

where τ_{ij} = stress in the x_j direction on a surface normal to the x_i direction

$\Delta \overline{M}_j$ = momentum transferred in the x_j direction

f = collision frequency/2

p_i = number of spheres per unit area normal to the x_i direction.

The formulation of stresses expressed in eq 4 does not incorporate the fact that there are two kinds of spheres, in which case we consider the control volume shown in Figure 2. Stresses are produced by four different kinds of collisions. The correct form of eq 4 for a two-size mixture is thus

$$\tau_{ij} = \sum_{P,Q} \Delta \overline{M}_{PQ_j} \cdot \frac{N^s_{PQ}}{2} \cdot p_{Pi} \tag{5}$$

e $\Delta \overline{M}_{PQ_j}$ is the momentum transfer in the x_j direction when a P-size and a Q-size sphere collide (P,Q can be large or small as denoted by L or S), N^s_{PQ} is the frequency of collisions any given P-size sphere receives from Q-size particles, and p_{Pi} is the number of P-size spheres on a unit area normal to the x_i direction.
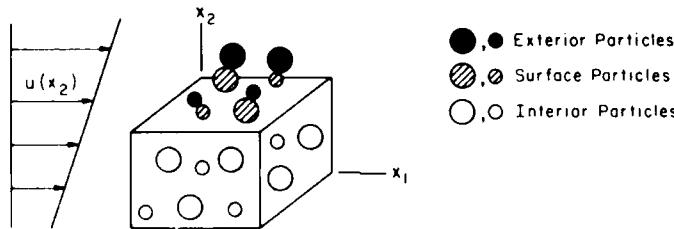

Figure 2. A control volume in a granular flow of uniform spheres.

$$\frac{\text{shear stress (two-size with spectrum given by Figure 3b)}}{\text{shear stress (single-size with spectrum given by Figure 3a)}} = \frac{1}{2.5} .$$

It is worthwhile noting that in all the stress computations, $C_o = 0.74$ was used. This value of C_0 corresponds to the hexagonal dense packing of single-size spheres. In a granular material, the densest state in which all neighboring spheres are touching may not exhibit the hexagonal structure. Moreover, the existence of more than one size in the flowing assembly can further vary the value of C_0. The effect of size distribution on the value of C_0 has been studied (e.g. McGaw 1967, Visscher and Bolsterli 1972), but is not sufficiently understood for the purpose of this work. Further study is needed to incorporate the variability of C_0 as a function of the size distribution.

As an example, the results shown in eq 50a and 56a are applied to the log-normal distributions

$$P(D) = \frac{1}{\sqrt{2\pi}\, oD} \exp\left(-\frac{1}{2}\left(\frac{\ln D - \eta}{\sigma}\right)^2\right) .$$
(57)

The result is shown in Figure 8 with $\eta = 0$, $D_{min} = e^{\eta - 3\sigma}$, $D_{max} = e^{\eta + 3\sigma}$ and

$$\tilde{\tau} = \tau_{21}(\text{log-normal})/\tau_{21}(D_M)$$

where D_M is the mean size of the log-normal distribution and the shear stress $\tau_{21}(D_M)$ is computed assuming a single-size assembly (Shen and Ackermann 1982, 1984).


Figure 8. The effect of log-normal size distribution on the shear stresses in a simple shear flow of spheres or disks.
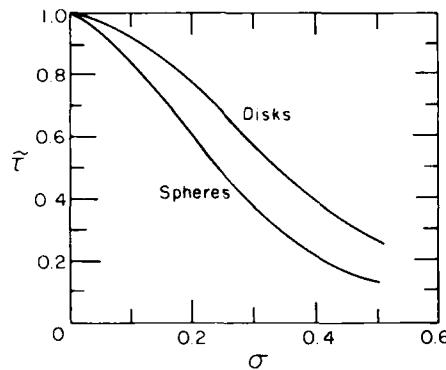
CONCLUSION

Theoretical analysis of the stress–strain-rate relationships for rapid granular flows have been limited to single-size assemblies of spheres or disks. Extension to an assembly with an arbitrary size distribution is needed for analyzing real granular materials. A study was carried out for a two-size mixture of spherical particles (Shen 1985). In that study, assumptions were made that restrict the applicability of the result to cases when the size ratio is nearly 1.

Two studies are made in this report. First, the stress–strain-rate relationship is established for a binary spherical assembly at the other extreme, namely, as the ratio of the two sizes is nearly 0. With the combination of the two extreme cases when the size ratio is nearly 1 or 0, a smoothing technique is used to give an approximate stress state for any intermediate size ratio. Hence, the constitutive equations for a binary assembly of spheres of an arbitrary size ratio are obtained. Second, an arbitrary spectrum of size distribution is incorporated into the analysis. The effect of size distribution of the stresses is quantified for both the sphere-shaped and the disk-shaped particles. The result demonstrates a reduction of stresses as the size gradation broadens. This phenomenon may explain some of the observations from earlier experimental work on sediment transport.

As indicated earlier in this report, further work is needed to improve the derivation for the average gap between neighboring spheres, since the densest solid concentration, although assumed here to be a constant, is a function of the size distribution. This is true for both mixtures of two sizes and of a complete size spectrum. The explicit form of this function is unknown yet.

Also, in the case of a complete spectrum of sizes, as the size gradation widens, the larger particles' fluctuations reduce to zero because of the equipartition of energy. In this case, the analysis has to be modified to reevaluate the dynamic interactions involving larger particles. For a binary mixture, this modification has been carried out in this report. However, it is not clear how to proceed along this line for a general spectrum of sizes. Nevertheless, based on the result of a binary

17

$$\Delta M_{DD'1} = \frac{\rho_s d}{6}(1+\epsilon)\frac{du}{dx_2}\left(\frac{D+D'}{2}+s\right)\frac{D^2 D'^2}{D^2+D'^2} \tag{52a}$$

$$\Delta M_{DD'2} = \frac{\rho_s d}{\pi}(1+\epsilon)\sqrt{v_D'^2 + v_{D'}'^2}\,\frac{D^2 D'^2}{D^2+D'^2} \tag{52b}$$

$$E_{DD'} = \rho_s\frac{\pi d}{4}\left(\frac{1-\epsilon^2}{4}+\frac{\mu(1+\epsilon)}{\pi}-\frac{\mu^2(1+\epsilon)^2}{4}\right)(v_D'^2+v_{D'}'^2)\frac{D^2 D'^2}{D^2+D'^2}\ . \tag{52c}$$

The equipartition of energy becomes

$$D^2 v_D'^2 = D'^2 v_{D'}'^2\ . \tag{53}$$

Substituting eq 41d, 51a–d, 52a and c into eq 47, we obtain

$$v_D'^2 D^2 = \frac{2k(\frac{du}{dx_2})^2\iint\left(\frac{D+D'}{2}+s\right)\frac{C_D C_{D'}}{D^2+D'^2}\frac{1}{D'}dD'dD}{\iint\frac{C_D C_{D'}}{D^3 D'^3}\,dD'dD} \tag{54}$$

where

$$k = \frac{1+\epsilon}{3\pi\left(\frac{1-\epsilon^2}{4}+\frac{\mu(1+\epsilon)}{\pi}-\frac{\mu^2(1+\epsilon)^2}{4}\right)}. \tag{55}$$

The shear and normal stresses are computed by substituting eq 41d, 51a and c and 52a and b into eq 39:

$$\tau_{21} = \rho_s\frac{1+\epsilon}{3\pi}\frac{du}{dx_2}\frac{\iint\left(\frac{D+D'}{2}+s\right)\frac{D}{s}C_D C_{D'}\frac{D/D'}{D^2+D'^2}v_D'^2\,dD'dD}{\int\frac{C_D v_D'}{D^2}\,dD} \tag{56a}$$

$$\tau_{22} = -\rho_s\frac{2(1+\epsilon)}{\pi^2}\frac{\iint\frac{(D/D')^2}{\sqrt{D^2+D'^2}}C_D C_{D'}v_D'^3\,dD'dD}{s\int\frac{C_D}{D^2}v_D'\,dD} \tag{56b}$$

where v_D' is defined in eq 54 and s is defined in eq 51d.

When $P(D)$ equals the Dirac delta function $\delta(D)$, eq 50a and b and 56a and b reduce to the stresses for a single-size sphere or disk assembly as given by Shen and Ackermann (1982*, 1984).

If eq 50a is used for a complete spectrum of sizes to reevaluate the comparison between the theory and the experimental data obtained by Savage and Sayed (1980) discussed previously, the new theory gives

---

*Because of an underestimation of two particles' relative fluctuation, the calculated stresses for spheres should have been $1/\sqrt{2}$ of what were shown by Shen and Ackermann (1982).

If eq 41–46 are substituted into eq 47, the fluctuation speed for the mean size D_M is obtained:

$$v'^2_{DM} = \frac{2k(\frac{du}{dx_2})^2 \iint (\frac{D+D'}{2} + s) \frac{C_D C_{D'}}{D^3 + D'^3} (DD'^3)^{-\frac{1}{2}} dD'dD}{D_M^3 \iint C_D C_{D'} (DD')^{-9/2} dD'dD} \tag{48}$$

where

$$k = \frac{(1+\epsilon)(0.05 + 0.08\,\mu)}{\frac{1-\epsilon^2}{4} + \frac{\mu(1+\epsilon)}{\pi} - \frac{\mu^2(1+\epsilon)^2}{4}} \tag{49}$$

For any given size between D and $D+dD$, the fluctuation speed can be derived using eq 46 and 48.

After substituting eq 41c and d, 43a and b, 46 and 48 into eq 39, the shear stress τ_{21} and normal stress τ_{22} in a simple shear flow of spheres are

$$\tau_{21} = \rho_s(1+\epsilon)(0.05 + 0.08\,\mu)\frac{du}{dx_2} \frac{\iint (\frac{D+D'}{2} + s)\frac{D}{s} C_D C_{D'} \frac{(D/D')^{3/2} v'^2_D}{D^3 + D'^3} dD'dD}{\int \frac{C_D}{D^3} v'_D dD} \tag{50a}$$

$$\tau_{22} = -\rho_s \frac{2(1+\epsilon)}{\pi^2} \frac{\iint \frac{D}{s} \frac{(D/D')^{3/2}}{\sqrt{1+(D/D')^3}} \frac{C_D C_{D'}}{D'^3} v'^3_D dD'dD}{\int \frac{C_D}{D^3} v'_D dD} . \tag{50b}$$

These were computed with a PC Zenith–100 using a program written in PASCAL. The computation only takes a few seconds to run for all the distribution functions tested.

Based on the analysis of a planar, simple shear flow of a single-size disk assembly (Shen and Ackermann 1984), the above analysis for a spherical assembly can easily be extended to a disk-shaped material with a uniform thickness. Consider a layer of disks with uniform thickness d and a distribution of diameters as given in Figure 7a or 7b. This layer of disks is undergoing a simple shear flow in its own plane. Equation 39 can be applied directly to evaluate the stresses generated by disk–disk collisions. Using the notations defined before, this time for a disk-shaped assembly,

$$G_D = \frac{C_D/D^2}{\int C_D/D^2 dD} \tag{51a}$$

$$N_D = \frac{4}{\pi} \frac{C_D}{D^2 d} \tag{51b}$$

$$P_D = \frac{4}{\pi} \frac{C_D}{Dd} \tag{51c}$$

$$s = R(\frac{C_D}{C})^{\frac{1}{2}} - R \tag{51d}$$

where R is defined in eq 42b, and

15

$$G_D = \frac{C_D/D^3}{\int C_D/D^3\, dD} \tag{41a}$$

$$N_D = \frac{6}{\pi}\frac{C_D}{D^3} \tag{41b}$$

$$P_D = \frac{6}{\pi}\frac{C_D}{D^2} \tag{41c}$$

$$N^s_{DD'} = \frac{G'_D v'_D}{\int G_D v'_D\, dD} \cdot \frac{v'_D}{s} \tag{41d}$$

where

$$s = R\left(\frac{C_o}{C}\right)^{1/3} - R \tag{42a}$$

and

$$R = \iint G_D G'_D \; \frac{D+D'}{2} \; dD'dD . \tag{42b}$$

The average momentum transfer and energy dissipation are

$$\Delta M_{DD'_1} = \Delta \vec{M}_{DD'} \cdot \vec{i} = \rho_s \frac{\pi}{6}(1+\epsilon)(0.05 + 0.08\,\mu)\,\frac{du}{dx_2}\left(\frac{D+D'}{2} + s\right)\frac{2D^3 D'^3}{D^3+D'^3} \tag{43a}$$

$$\Delta M_{DD'_2} = \Delta \vec{M}_{DD'} \cdot \vec{j} = -\rho_s \frac{2}{3\pi}(1+\epsilon)\sqrt{v'^2_D + v'^2_{D'}}\,\frac{D^3 D'^3}{D^3+D'^3} \tag{43b}$$

$$E_{DD'} = \rho_s \frac{\pi}{6}\left(\frac{1-\epsilon^2}{4} + \frac{\mu(1+\epsilon)}{\pi} - \frac{\mu^2(1+\epsilon)^2}{4}\right)(v'^2_D + v'^2_{D'})\frac{D^3 D'^3}{D^3+D'^3} \tag{43c}$$

The equipartition of energy takes the same form as before:

$$D^3 v'^2_D = D'^3 v'^2_{D'} . \tag{44}$$

Given an arbitrary size distribution designated by some probability density function $P(D)$, the mean size D_M is

$$D_M = \int D P(D) dD . \tag{45}$$

The fluctuation speed for this mean size is

$$v'^2_{DM} = v'^2_D \left(\frac{D}{D_M}\right)^3 . \tag{46}$$

The energy balance equation, eq 9, now takes the form

$$\frac{du}{dx_2}\iint \Delta M_{DD'_1}\,\frac{N^s_{DD'}}{2}\,P_D dD'dD = \iint E_{DD'}\,N_D\,\frac{N^s_{DD'}}{2}\,dD'dD . \tag{47}$$

14
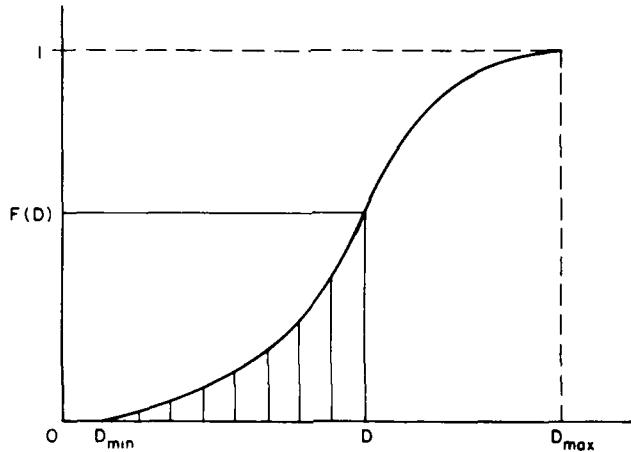
a. *Probability distribution.*
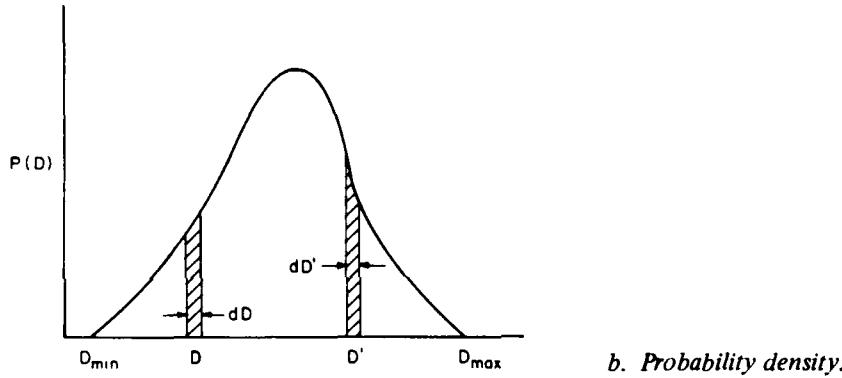
b. *Probability density.*

Figure 7. Particle size distribution.

$$\Delta \vec{M}_{DD'} \; \frac{N^s_{DD'}}{2} \; dD' \; P_D dD \; . \tag{38}$$

Hence the total stress caused by all possible collisions is

$$\iint \Delta \vec{M}_{DD'} \; \frac{N^s_{DD'}}{2} \; dD' \; P_D dD \tag{39}$$

with the integration limits defined by the range of size under consideration.

If the results obtained in the previous section for two discrete sizes are applied to the present case of a continuous size distribution, the quantities in the above notation list are (with the understanding that all integrals are taken from the minimum diameter to the maximum diameter)

$$C_D = P(D) \cdot C \tag{40}$$

where $P(D)$ is the given probability density function of the size distribution,

13
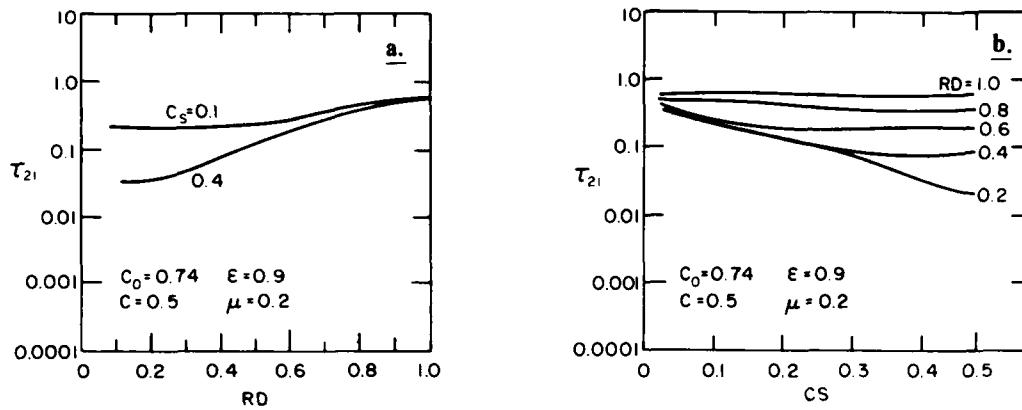
Figure 6. Shear stress in a simple shear flow of spheres of two sizes.

By use of the revised theory of a two-size mixture, the comparison between the theoretical prediction and experimental data obtained by Savage and Sayed (1984) becomes

$$\frac{\text{shear stress (two-size given by eq 37 with } n = 3)}{\text{shear stress (single-size given by eq 13a)}} = \tfrac{1}{2} \ .$$

COMPLETE SPECTRUM ANALYSIS FOR SPHERES AND DISKS

Based on the analysis for a two-size mixture, stresses can now be obtained for mixtures with any size distribution. A typical size distribution in a natural material is shown in Figure 7a, where $F(D)$ is the cumulative volume percentage of spheres that have sizes up to D.

The derivative of $F(D)$ is denoted by $P(D)$ as shown in Figure 7b. The volume fraction of spheres that have sizes between D and $D+dD$ is represented by $P(D)dD$. The results obtained previously for a binary mixture can be directly transferred to this complete spectrum analysis. The two discrete sizes D_L and D_S are replaced by two differential size ranges: D to $D+dD$ and D' to $D'+dD'$. The spectra for both D and D' are the same and are determined by the probability distribution function $F(D)$ or the probability density function $P(D)$.

The following notations will be used in the succeeding discussions:

C	= total volume concentration of all spheres
$C_D dD$	= volume concentration of spheres with diameters D to $D+dD$
$G_D dD$	= number percentage of particles with diameters D to $D+dD$
$N_D dD$	= number of spheres in a unit volume with diameters D to $D+dD$
$P_D dD$	= number of spheres with diameters D to $D+dD$ on a unit surface
$N^s_{DD'} dD'$	= frequency of collisions a D-size sphere receives from all the spheres with diameters D' to $D'+dD'$
$\Delta M_{DD'}$	= average momentum transfer between two spheres of diameters ranging from D to $D+dD$ and D' to $D'+dD'$
$E_{DD'}$	= average energy dissipation because of a collision between spheres with diameters D to $D+dD$ and D' to $D'+dD'$
v'_D	= fluctuation speed of spheres with diameters D to $D+dD$
s	= average gap between adjacent spheres.

Using the notation above, we see that the rate of momentum transfer across a unit surface because of collisions between spheres of diameters D to $D+dD$ and D' to $D'+dD'$ is

12
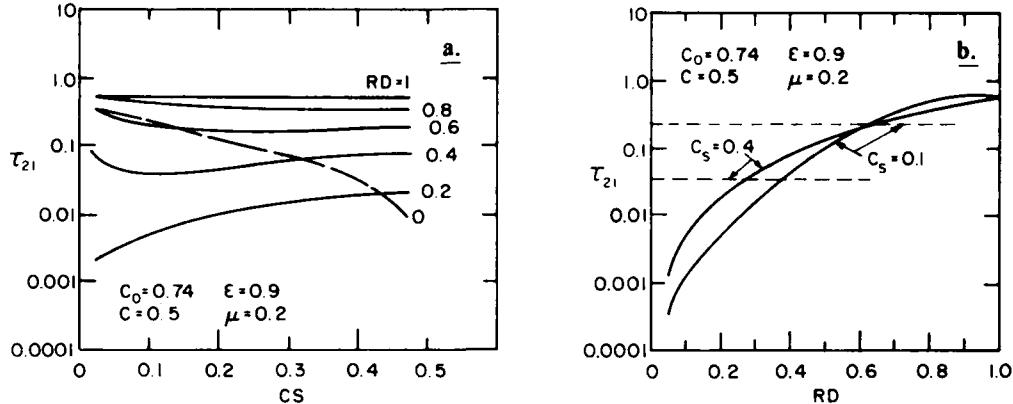
Figure 5. Asymptotic solutions for shear stress in a simple shear flow of spheres of two sizes (dashed lines = RD → 0, solid lines = RD → 1).

fluctuations are not negligible. However, this analysis gives a possible condition under which Bagnold's assumption is valid: when large spheres are sheared in dust-like material, the large spheres only move with the mean flow and the resulting stresses have the same characteristics as those formulated by Bagnold (1954). Equation 36b also shows that as μ increases from 0 to 4/7, a reversal of τ_{22} from negative to positive occurs. It is believed that if particle rotations due to the frictional impact are included in the analysis, such reversal will be removed and τ_{22} will stay negative.

In general, as the shearing spheres decrease in size, the stresses decrease too. Equations 36a and b are derived for the case when RD approaches 0 while C_S and C_L are fixed, therefore they set up a lower bound for the stresses in a binary mixture. For a given set of C_S, C_L and D_L, as D_S approaches 0, the stresses must reduce monotonically.

Equations 13a and 36a are plotted in Figure 5 where the general behavior of the shear stress for $0 < RD < 1$ is depicted. The dashed curves are from eq 36a, which represent the case as RD approaches 0; the solid curves are from eq 13a, which is applicable as RD approaches 1.

An analytical formulation of the stresses for an arbitrary RD is difficult. However, with the two limiting cases quantified in Figure 5, smoothing procedures as discussed by Churchill and Usagi (1972) can be used to combine the two curves into one curve that describes the stresses for the entire range of RD. A possible way to join the two limiting cases is given as:

$$\tau_{ij}^n (RD) = \tau_{ij_0}^n (RD) + \beta \tau_{ij_1}^n (RD) \tag{37a}$$

where

$$\beta = 1 - \left(\frac{\tau_{ij_0(1)}}{\tau_{ij_1(1)}} \right)^n \tag{37b}$$

and τ_{ij_0} are the stresses given by eq 36a and b, which correspond to $RD \to 0$, and τ_{ij_1} are the stresses given by eq 13a and b, which correspond to $RD \to 1$. The larger n is, the closer τ_{ij} follows the limiting values of τ_{ij_0} and τ_{ij_1}. Equation 37 approximates the stresses for a two-size mixture of any $0 < RD < 1$. $\tau_{21} (RD)$ is plotted in Figure 6 with $n = 3$. It was found that for $n > 3$, the solution given in eq 37 remains independent of n up to the second decimal place.

11

$$\tau_{21} = \rho_s \frac{D_L^3}{\pi} (1+\epsilon)(0.05 + 0.08\,\mu)\frac{du}{dx_2}\left[\left(\frac{D_L + s_L}{D_L}\right)^2 \frac{D_L}{s_L}\frac{du}{dx_2} + 3\frac{D_S}{D_L}\frac{C_L C_S}{D_L}\frac{v_S'}{s_S}\right] \tag{31a}$$

$$\tau_{22} = \rho_s \frac{D_L^3}{\pi} (1+\epsilon)(-0.07 + 0.04\,\mu)\frac{du}{dx_2}\left(\frac{D_L + s_L}{D_L}\right)^2 \frac{C_L}{s_L} \tag{31b}$$

in which the terms involving the square and higher powers of RD are dropped. The energy dissipation in a pair of like spheres' collision is

$$E_{LL} = \rho_s \frac{\pi D_L^3}{6}\left(\frac{du}{dx_L}\right)^2 \left(\frac{D_L + s_L}{2}\right)^2 \left(\frac{1-\epsilon^2}{4} + \frac{\mu(1+\epsilon)}{\pi} - \frac{\mu^2(1+\epsilon)^2}{4}\right) \tag{32}$$

where collisions are assumed to occur with relative velocity determined strictly by the mean flow, and

$$E_{SS} = \rho_s \frac{\pi D_S^3}{6}\, v_S'^{\,2}\left(\frac{1-\epsilon^2}{4} + \frac{\mu(1+\epsilon)}{\pi} - \frac{\mu^2(1+\epsilon)^2}{4}\right) \tag{33}$$

where collisions are assumed to occur at relative fluctuation velocity. Since the large spheres have infinite mass compared with the small spheres, we have

$$E_{LS} = E_{SS}\,. \tag{34}$$

Substituting eq 10, 23, 27, 31a, 32, 33 and 34 into eq 9, we obtain v_S' as

$$v_S' = \left(\frac{\frac{1+\epsilon}{2}(0.05 + 0.08\,\mu)\left(\frac{D_L + s_L}{D_L}\right)^2 \frac{C_L}{s_L} - \frac{1}{4}\left[\frac{1-\epsilon^2}{4} + \frac{\mu(1-\epsilon)}{\pi} - \frac{\mu^2(1+\epsilon)^2}{4}\right]\left(\frac{D_L + s_L}{D_L}\right)^3 \frac{C_L}{s_L}}{\frac{C_S}{s_S}\frac{1-\epsilon^2}{4} + \frac{\mu(1+\epsilon)}{\pi} - \frac{\mu^2(1+\epsilon)^2}{4}}\right)^{1/3}$$

$$\cdot\, D_L \frac{du}{dx_2}\,. \tag{35}$$

The shear and normal stresses are thus obtained after substituting eq 35 into eq 31a and b and setting D_S/D_L equal to zero,

$$\tau_{21} = \rho_s C D_L^2 \left(\frac{du}{dx_2}\right)^2 (1+\epsilon)(0.05 + 0.08\,\mu)\frac{C_L^{2/3}\,C_o^{2/3}}{\pi C(C_o^{1/3} - C_L^{1/3})} \tag{36a}$$

$$\tau_{22} = \frac{-0.07 + 0.04\,\mu}{0.05 + 0.08\,\mu}\,\tau_{21}\,. \tag{36b}$$

An interesting observation is that τ_{21}/τ_{22} is only a material constant now, independent of the solid concentration. This phenomenon is quite different from the result when RD approaches 1 as shown in eq 13a and b. Bagnold (1954) derived the stresses assuming that single-size spheres do not fluctuate while being sheared in a Newtonian fluid. His result also demonstrated that τ_{21}/τ_{22} is independent of the solid concentration. Experiments show that velocity fluctuations do exist in the shearing flow of a nearly single-size solid–fluid mixture and previous analysis, which includes velocity fluctuations, shows that τ_{21}/τ_{22} does depend on solid concentration (Shen and Ackermann 1982), hence Bagnold's result does not describe the flow when velocity

$$C_{Sa} = C_S/(1 - C_L). \tag{24}$$

Let C_{So} denote the densest concentration of the fine spheres,

$$\frac{C_{Sa}}{C_{So}} = \left(\frac{D_S}{D_S + s_S}\right)^3. \tag{25}$$

After substituting eq 24 into eq 25 and solving for s_S,

$$s_S = D_S \left((C_{So}/C_{Sa})^{1/3} - 1\right). \tag{26}$$

Let N_{SL}^s be the frequency of collisions between a small sphere and the surrounding large spheres. The total number of collisions between large and small spheres is equal to the product of N_{LS}^s and the number of large spheres and also equal to the product of N_{SL}^s and the number of small spheres, therefore,

$$N_{SL}^s = N_{LS}^s \frac{C_L}{C_S} \left(\frac{D_S}{D_L}\right)^3. \tag{27}$$

When a small sphere being considered is not adjacent to a large sphere, the collision frequency between a small sphere and the surrounding small spheres is

$$N_{SS}^s = v_S'/s_S. \tag{28}$$

If the small sphere being considered is adjacent to a large sphere, then only half of the collisions of the small spheres are with small ones; the other half are with large ones. However, since the number of small spheres minus the number of small spheres adjacent to large spheres, or

$$\frac{6C_S}{\pi D_S^3} - \frac{6C_S}{\pi D_S^2} \pi D_L^2 \frac{6C_L}{\pi D_L^3} = \frac{6C_S}{\pi D_S^3} \left(1 - \frac{D_S}{D_L} \ 6 \ C_L\right) \rightarrow 6C_S/\pi D_S^3 \ \text{ as } D_S/D_L \rightarrow 0$$

the above result indicates that as D_S/D_L approaches 0, almost all the small spheres are surrounded by only small spheres. Hence, eq 28 is a good approximation of the collision frequency between any small sphere and its surrounding small spheres.

As discussed earlier, as RD approaches 0, v_L' approaches 0 and large spheres follow the mean flow motion. In this case the momentum transfer in both the x_1 and x_2 directions in a collision of two large spheres is a result of the relative motion from the mean velocity gradient only. Hence,

$$\Delta M_{LL1} = \rho_s \frac{\pi D_L^3}{6} (1+\epsilon)(0.05 + 0.08 \mu)(D_L + s_L)\frac{du}{dx_2} \tag{29}$$

which is the same as eq 6a in the previous section, and

$$\Delta M_{LL2} = \rho_s \frac{\pi D_L^3}{6} (1+\epsilon)(0.07 + 0.04 \mu)(D_L + s_L)\frac{du}{dx_2} \tag{30}$$

which is obtained by averaging the momentum transfer induced by the mean flow in the x_2-direction (while eq 6b was obtained by averaging momentum transfer induced by the fluctuation in the x_2-direction). Substituting eq 21, 23, 27, 28 and 29 into eq 5, we obtain the shear and normal stresses in terms of the unknown v_S',

9

centration of large spheres C_L, the average gap between two adjacent large spheres can be computed from

$$\frac{C_L}{C_{Lo}} = \left(\frac{D_L}{D_L + s_L}\right)^3 \tag{18}$$

where C_{Lo} is the densest concentration of large spheres. Hence

$$s_L = D_L\left(\left(\frac{C_{Lo}}{C_L}\right)^{1/3} - 1\right). \tag{19}$$

The collision frequency between a large sphere and its neighboring large spheres, N_{LL}^s, is the ratio of their average relative velocity and their average gap size. It is shown in Appendix A that

$$N_{LL}^s = \frac{\displaystyle\int_{\pi/2}^{3\pi/2} \int_0^{\pi/2} \frac{du}{dx_2}(D_L + s_L)\cos\phi \; d\phi \, d\theta}{\displaystyle\int_{\pi/2}^{3\pi/2} \int_0^{\pi/2} -D_L \sin\phi \cos\theta + \sqrt{D_L^2 \sin^2\phi \cos^2\theta + (D_L + s_L)^2 - D_L^2} \; d\phi \; d\theta} \tag{20a}$$

where the following binomial expansion may be used for simplification,

$$\sqrt{D_L^2 \sin^2\phi \cos^2\theta + (D_L + s_L)^2 - D_L^2} = (D_L + s_L)\sin\phi \; \cos\theta$$

$$+ \frac{(1 - \sin^2\phi \cos^2\theta)(2D_L s_L + s_L^2)}{2\sqrt{(D_L + s_L)^2 \sin^2\phi \cos^2\theta}} + \cdots . \tag{20b}$$

When s_L/D_L is small, eq 20a reduces to

$$N_{LL}^s \approx \frac{\pi}{2} \frac{du}{dx_2} \frac{D_L + s_L}{s_L} . \tag{21}$$

This approximation overestimates N_{LL}^s if s_L/D_L is not very small, or equivalently, when large spheres become sparse.

Since large spheres do not fluctuate, the collision frequency between a large sphere in Figure 4 and the surrounding fine dust-like spheres is

$$N_{LS}^s = p_S \cdot A_L \cdot \frac{f_S}{2} \tag{22}$$

where p_S is the number of fine spheres per unit area in the flow field, A_L is the surface area of the large sphere, and f_S is the frequency of fluctuations of a fine sphere. Hence

$$N_{LS}^s = 3C_S \left(\frac{D_L}{D_S}\right)^2 \frac{v_S'}{s_S} \tag{23}$$

where s_S is the gap between two adjacent fine spheres. Rather than assuming that the average gap between small spheres is the same as that between large spheres as was done in the previous section, a more realistic model will be pursued as follows, which applies to the case when RD approaches 0. Since the available volume for the fine spheres is $1 - C_L$, the actual concentration of the fine spheres that fill the interstice of the large spheres is

8
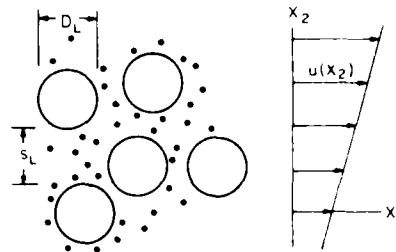
Figure 4. Simple shear flow of spheres in dust-like material.

In the limiting case as RD approaches 0, it is no longer reasonable to assume that the mean gap between small spheres is the same as that between the large ones. Most importantly, in this limit the equipartition of fluctuation energy defined in eq 12 forces v'_L to approach 0. The equipartition of fluctuation energy still applies as RD approaches 0. However, the collision frequency needs to be modeled differently in this case, as will be explained below.

As modeled previously, the collision frequency is calculated as the ratio of v' and the mean gap size between spheres. Therefore, when v'_L approaches 0, the collision frequencies involving large spheres approach 0. The stress, which is now obtained by collisions between small spheres, is proportional to D_S^2. Hence when RD approaches 0, the stresses approach 0 (see Figure 5a in Shen [1985]). This result contradicts reality, however, since when the concentration of large spheres is high, the existing mean shear as shown in Figure 1 must result in collisions whether particles fluctuate or not. In fact, the collision frequency between neighboring spheres, if modeled rigorously, should be a function of both the velocity of fluctuation and the relative mean velocity ascribable to the mean shear flow. It is when the fluctuation speed is much higher than the relative mean velocity that the collision can be modeled as a result of fluctuations only. As RD approaches 0, v'_L approaches 0 and the collisions between large spheres become a result of the relative mean shear velocity alone.

In the limiting case as RD approaches 0, we may view the two-component system as an assembly of large spheres sheared in a highly energy-absorbing material. As illustrated in Figure 4, this material consists of numerous fine dust-like particles that are fluctuating and spherical. These fine particles collide with each other and the large spheres. The large spheres, driven by the mean shear motion, occasionally collide with neighboring large spheres. The collisions between large spheres cause them to temporarily deviate from the local mean motion. From the energy point of view, this temporary deviation of the large spheres' velocity produces a fluctuation energy in them. Because of the equipartition of energy, this temporary imbalance of fluctuation energy is absorbed by the surrounding fine dust particles. As RD approaches 0 the amount of energy dissipated per collision between the large and small spheres remains the same as described by eq 11b and 12. However, as C_S/C_L is kept constant, and as RD approaches D, the number of the fine particles surrounding the large spheres increases as RD^{-3}. The fluctuation speed of the small spheres and the collision frequencies increase as $RD^{-3/2}$. Hence the time scale of absorbing this energy imbalance decreases as $RD^{9/2}$. Therefore, as RD approaches 0, the large spheres' motion reduces to the local mean velocity long before the next collision between the large spheres takes place. In this limiting case, the collision frequency between large and small spheres, which is the main factor of the stress generation, is no longer a function of v'_L, but rather a function of the mean velocity gradient alone.

Consider randomly distributed large spheres sheared as shown in Figure 4, with the interstice filled with small spheres with diameter D_S approaching 0. The large spheres travel strictly with the mean flow. The average collision frequency between a large sphere and the surrounding large spheres is

$$N^s_{LL} = \overline{V}_L/s_L \tag{17}$$

where $\overline{V}_L$ is the average relative velocity between two adjacent large spheres and s_L is the average gap between two adjacent large spheres. In a random assembly of large spheres, with a given con-

7
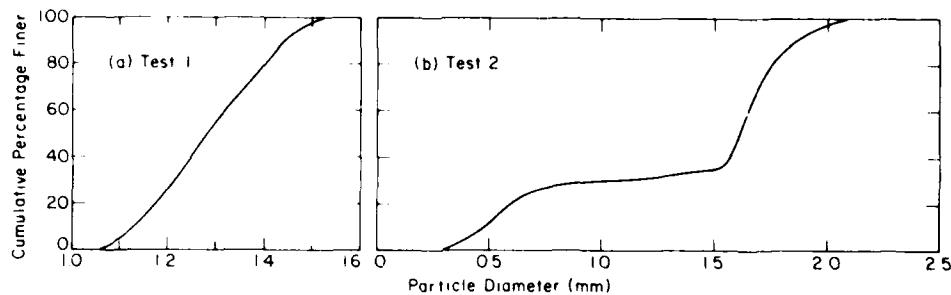
Figure 3. Particle size distribution of spheres (after Sayed 1981).

where

$$RD = D_S/D_L \quad , \quad RC = C_S/C_L \tag{14}$$

$$F = RD^{-1} + f_s + (1+f_s)\ RC^2 RD^{-5} + \frac{RC \cdot RD^{-7/2}}{1+RD^{-3}}\ (1+RD^{-1}+2f_s)(1+RD^{-1}) \tag{15}$$

and

$$f_S = \frac{RD^2 + RC}{RD^3 + RC}\ \frac{C_o^{1/3} - C^{1/3}}{C^{1/3}} \ . \tag{16}$$

We now compare the model with two tests conducted by Savage and Sayed (1984). Test 1 used nearly uniform plastic beads with a mean diameter of 1.32 mm. Test 2 used a 7:3 mixture of of the same material with mean diameters of 1.65 mm and 0.6 mm. The weighted mean of the two sizes is 1.34 mm. The size distributions for test 1 and test 2 are given in Figure 3 (Sayed 1981). The ratio of the shear stresses obtained in these two materials was measured to be

shear of test 2/shear of test 1 = 1/4.5 .

The theoretical result according to eq 13 is

shear of test 2/shear of test 1 = 1/10 .

This comparison shows that the theoretical prediction is in the right order of magnitude; however, it is apparent from Figure 3 that the size spectrum in test 1 and the two individual spectra in test 2 are not very narrow. The above comparison will be revised after the analysis for a continuous size distribution is completed.

LIMITING CASE OF THE TWO-SIZE MIXTURE

At the time when the analysis in *Part 1: Two Grain Sizes* (Shen 1985) was carried out, this author was not aware that the geometry and kinematics of the granular assembly as RD approaches 0 is very different from the case when RD approaches 1, as will be discussed in detail later. An implicit assumption in the analysis in *Part 1* is that RD approaches 1. Modified constitutive qua-tions that relax this assumption are derived in this section. These modified constitutive equations are obtained by combining the result shown in the previous section, which applies to the case when RD approaches 1, and the result for the case as RD approaches 0.

6

$$\tau_{21} \frac{du}{dx_2} = N_{LS} \overline{E}_{LS} + N_{LL} \overline{E}_{LL} + N_{SS} \overline{E}_{SS} \tag{9}$$

where N_{PQ} (P and $Q = L$ or S) is the frequency of all collisions between a P-size and a Q-size sphere in a given unit volume and $\overline{E}_{PQ}$ is the average energy dissipated in a collision between P-size and Q-size spheres. By definition,

$$N_{LS} = N_L \, N_{LS}^s \tag{10a}$$

$$N_{LL} = N_L \, \frac{N_{LL}^s}{2} \tag{10b}$$

$$N_{SS} = N_S \, \frac{N_{SS}^s}{2} \; . \tag{10c}$$

The average energy dissipation in each of the three different kinds of collisions is derived as (Shen 1985):

$$\overline{E}_{LL \text{ or } SS} = \rho_s \, \frac{\pi D_L^3}{6} \, v'^2_{L \text{ or } S} \, [\frac{1-\epsilon^2}{4} + \frac{\mu(1+\epsilon)}{\pi} - \frac{\mu^2(1+\epsilon)^2}{4}] \tag{11a}$$

$$\overline{E}_{LS} = \rho_s \, \frac{\pi D_L^3}{6} \, \frac{v'^2_L + v'^2_S}{1 + (\frac{D_L}{D_S})^3} \, [\frac{1-\epsilon^2}{4} + \frac{\mu(1+\epsilon)}{\pi} - \frac{\mu^2(1+\epsilon)^2}{4}] \; . \tag{11b}$$

To relate v'_L and v'_S, an equipartition of energy is assumed. Then

$$D_L^3 v'^2_L = D_S^3 v'^2_S \tag{12}$$

namely, the energy contained in the fluctuational motion of the large and small spheres is the same (the justification of this assumption is given by Shen 1985).

After assembling eq 6-12 into eq 5, the stresses for a mixture of two sizes of spheres are obtained as

$$\tau_{21} = C\rho_s D_L^2 (\frac{du}{dx_2})^2 \, \frac{(1+\epsilon)^{3/2} (0.053+0.081\,\mu)^{3/2}}{[\frac{1-\epsilon^2}{4} + \frac{\mu(1+\epsilon)}{\pi} - \frac{\mu^2(1+\epsilon)^2}{4}]^{1/2}} \cdot \frac{[1+(RC)\,RD^{-3}]\,C^{1/3}}{2[1+(RC)\,RD^{-2}]\,(C_o^{1/3} - C^{1/3})}$$

$$\cdot \frac{F^{3/2}}{[1+(RC)\,RD^{-9/2}]^2} \cdot \frac{1}{1+RC} \tag{13a}$$

$$\tau_{22} = -\tau_{21} \, \frac{(1+\epsilon)^{1/2}}{(0.053+0.081\,\mu)^{1/2} \, [\frac{1-\epsilon^2}{4} + \frac{\mu(1+\epsilon)}{\pi} - \frac{\mu^2(1+\epsilon)^2}{4}]^{1/2}} \, \frac{1}{\pi^2 F^{1/2}}$$

$$\cdot [2\sqrt{2}\,(RD^{-1} + RC^2 RD^{-13/2}) + 4\,\frac{RC(RD)^{-4} + RC(RD)^{-3}}{(1+RD^3)^{1/2}}] \tag{13b}$$

5

These three quantities—$\Delta \overline{M}_{PQ_j}$, N^s_{PQ} and p_{P_j}—are derived as (Shen 1985):

$$\Delta \overline{M}_{LL1} = \rho_s \frac{\pi D_L^3}{6} \, (1+\epsilon) \, (0.053 + 0.081 \, \mu) \frac{du}{dx_2} \, (D_L + s) \tag{6a}$$

$$\Delta \overline{M}_{LL2} = -\rho_s \, \frac{\pi D_L^3}{6} \, \frac{2(1+\epsilon)}{\pi^2} \, \sqrt{2} \; v'_L \tag{6b}$$

$$\Delta \overline{M}_{SS1} = \rho_s \, \frac{\pi D_S^3}{6} \, (1+\epsilon) \, (0.053 + 0.081 \, \mu) \frac{du}{dx_2} \, (D_S + s) \tag{6c}$$

$$\Delta \overline{M}_{SS2} = -\rho_s \, \frac{\pi D_S^3}{6} \, \frac{2(1+\epsilon)}{\pi^2} \, \sqrt{2} \; v'_S \tag{6d}$$

$$\Delta \overline{M}_{SL1} = \Delta \overline{M}_{LS1} = \rho_s \, \frac{\pi D_L^3}{6} \, (1+\epsilon) \, (0.053 + 0.081 \, \mu) \frac{du}{dx_2} \, \left(\frac{D_S + D_L}{2} + s \right) \frac{2 D_S^3}{D_S^3 + D_L^3} \tag{6e}$$

$$\Delta \overline{M}_{SL2} = \Delta \overline{M}_{LS2} = -\rho_s \, \frac{\pi D_L^3}{6} \, \frac{4}{\pi^2} \, \frac{(1+\epsilon) D_S^3}{D_S^3 + D_L^3} \, \sqrt{{v'_S}^2 + {v'_L}^2} \tag{6f}$$

where v'_L and v'_S are fluctuation speeds of the large and the small spheres respectively

$$N^s_{LL} = \frac{G_L v'_L}{GVT} \, \frac{v'_L}{s} \tag{7a}$$

$$N^s_{LS} = \frac{G_S v'_S}{GVT} \, \frac{v'_L}{s} \tag{7b}$$

$$N^s_{SL} = \frac{G_L v'_L}{GVT} \, \frac{v'_S}{s} \tag{7c}$$

$$N^s_{SS} = \frac{G_S v'_S}{GVT} \, \frac{v'_S}{s} \tag{7d}$$

$$GVT = G_L v'_L + G_S v'_S \tag{7e}$$

and

$$p_{L1 \text{ or } 2} = \frac{6 C G_L D_L}{\pi (G_L D_L^3 + G_S D_S^3)} \tag{8a}$$

$$p_{S1 \text{ or } 2} = \frac{6 C G_S D_S}{\pi (G_L D_L^3 + G_S D_S^3)} \; . \tag{8b}$$

Since the fluctuations are caused by the shearing motion, the work done by shear forces is the energy input for this mode of motion. On the other hand, the collisions produced by these fluctuations dissipate energy and this dissipation is the energy output for this mode of motion. When a steady state is established in the simple shear motion described in Figure 1, the energy input and output are balanced. In a mathematical form, this balance is presented as

4

mixture, it is believed that although the results given in eq 54 and 56 and Figure 8 underestimate the real stresses when the size gradation is very broad, the general trend of stress reduction as size gradation broadens is not going to be affected.

LITERATURE CITED

Ackermann, N.L. and H.H. Shen (1982) Stresses in rapidly sheared fluid-solid mixtures. *Journal of the Engineering Mechanics Division*, ASCE, 108(EM1): 95-113.

Bagnold, R.A. (1954) Experiments on gravity-free dispersion of large solid spheres in a Newtonian fluid under shear. *Proceedings of the Royal Society of London*, Ser. A, vol. 225, pp. 49-63.

Campbell, C.S. and C.E. Brennen (1983) Computer simulation of shear flows of granular material. *Mechanics of Granular Materials—New Models and Constitutive Relations* (J.T. Jenkins and M. Satake, editors). Amsterdam: Elsevier, pp. 313-326.

Churchill, S.W. and R. Usagi (1972) A general expression for the correlation of rates of transfer and other phenomena. *American Institute of Chemical Engineers Journal*, 18(6): 1121-1128.

Durand, R. (1953) Basic relationships of the transportation of solids in pipes—experimental research. *Proceedings, Minnesota International Hydraulics Convention*. International Association for Hydraulic Research, pp. 89-103.

Gilbert, G.K. (1914) Transportation of debris by running water. U.S. Geological Survey Professional Paper No. 86.

Jenkins, J.T. and S.B. Savage (1983) A theory for the rapid flow of identical, smooth, nearly elastic, spherical particles. *Journal of Fluid Mechanics*, 130: 187-202.

Kanatani, K.I. (1979) A micropolar continuum theory for the flow of granular materials. *International Journal of Engineering Science*, 17: 419-432.

Lun, C.K.K., S.B. Savage, D.J. Jeffrey and N. Chepurniy (1984) Kinetic theories for granular flow: Inelastic particles in couette flow and slightly inelastic particles in a general flowfield. *Journal of Fluid Mechanics*, 140: 223-256.

McGaw, R. (1967) Systematic packing from the standpoint of the primitive cell. USA Cold Regions Research and Engineering Laboratory, Research Report 201.

Ogawa, S., A. Umemura and N. Oshima (1980) On the equations of fully fluidized granular materials. *Zeitschrift für Angewandte Mathematick und Physik*, 31: 483-493.

Rothrock, D.A. (1975) The energetics of the plastic deformation of pack ice by ridging. *Journal of Geophysical Research*, 80(33): 4514-4519.

Savage, S.B. and M. Sayed (1984) Stresses developed by cohesionless granular materials sheared in an annular shear cell. *Journal of Fluid Mechanics*, 142: 391-430.

Sayed, M. (1981) Theoretical and experimental studies of the flow of cohesionless granular materials. Ph.D. dissertation. Montreal: McGill University.

Shen, H. (1985) Effect of nonuniform size on internal stresses in a rapid shear flow of granular materials. Part I: Two grain sizes. USA Cold Regions Research and Engineering Laboratory, CRREL Report 85-2.

Shen, H. and N.L. Ackermann (1982) Constitutive relationships for fluid-solid mixtures. *Journal of the Engineering Mechanics Division*, American Society of Civil Engineers, 108(EM5): 748-763.

Shen, H.H. and N.L. Ackermann (1984) Constitutive equations for a simple shear flow of a disc-shaped granular mixture. *Journal of Engineering Science*, 22(7): 829-843.

Visscher, W.M. and M. Bolsterli (1972) Random packing of equal and unequal spheres in two and three dimensions. *Nature*, 239: 504-507.

Walton, O.R. (1983) Particle-dynamics calculations of shear flow. *Mechanics of Granular Materials— New Models and Constitutive Relations* (J.T. Jenkins and M. Satake, editors). Amsterdam: Elsevier, pp. 327-338.

APPENDIX A: DERIVATION OF COLLISION FREQUENCY BETWEEN NEIGHBORING SPHERES THAT FOLLOW THE MEAN SHEAR FLOW WITHOUT FLUCTUATIONS

Let D be the diameter of spheres, and s be the average gap between neighboring spheres. Figure A1 shows the location of a sphere B. The inner dashed semi-sphere is the locus of the centers of neighboring spheres as a collision takes place on the surface of B. The outer dashed semi-sphere is the locus of the average centers of the neighboring spheres around B.
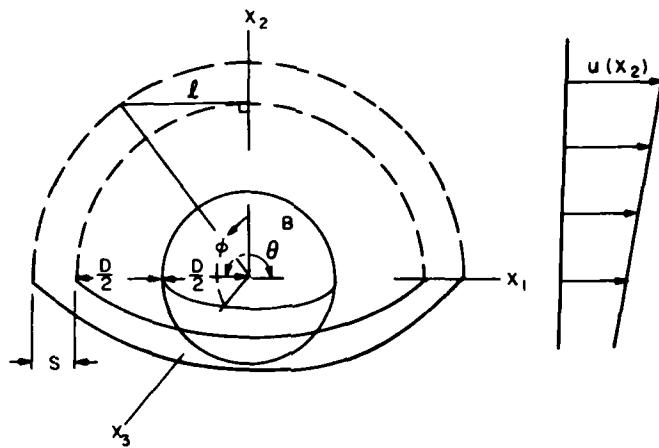
Figure A1. Geometry of a collision driven by mean flow.

The collision frequency between neighboring spheres is calculated as

$$\bar{u}/\bar{\ell} \tag{A1}$$

where $\bar{u}$ is the mean relative velocity between neighboring spheres and $\bar{\ell}$ is the mean distance traveled to make a collision contact. An example of a special ℓ is given in Figure A1.

When a sphere A collides with sphere B at

$$\vec{r} = r\sin\phi\cos\theta\,\vec{i} + r\sin\phi\sin\theta\,\vec{k} + r\cos\phi\,\vec{j}\ ; \ \frac{\pi}{2} \leqslant \theta \leqslant \frac{3\pi}{2}, 0 \leqslant \phi \leqslant \frac{\pi}{2}, |r| = D \tag{A2}$$

sphere A must have traveled, according to the mean relative velocity, a certain distance $\ell\vec{i}$. In Figure A1, $\vec{r} = D\vec{j}$. The mean location of sphere A before it started to move toward sphere B is, therefore,

$$\vec{R} = (r\sin\phi\cos\theta + \ell)\vec{i} + r\sin\phi\sin\theta\,\vec{k} + r\cos\phi\,\vec{j}\ ; \ |R| = D + s. \tag{A3}$$

Squaring eq A2 and A3, then subtracting one from the other, we find that

$$\ell = -D\sin\phi\cos\theta + \sqrt{D^2\sin^2\phi\cos^2\theta + (D+s)^2 - D^2}\ . \tag{A4}$$

The velocity of sphere A, which has moved this distance, is

$$u = \frac{du}{dx_2}(D+s)\cos\phi\ . \tag{A5}$$

19

Substituting eq A4 and A5 into A1, we calculate the collision frequency as

$$\frac{\displaystyle\int_{\pi/2}^{3\pi/2}\int_0^{\pi/2}\frac{du}{dx_2}(D+s)\cos\phi\,d\phi\,d\theta}{\displaystyle\int_{\pi/2}^{3\pi/2}\int_0^{\pi/2}-D\sin\phi\cos\theta+\sqrt{D^2\sin^2\phi\cos^2\theta+(D+s)^2-D^2}\,d\phi\,d\theta}. \tag{A6}$$

20

A facsimile catalog card in Library of Congress MARC
format is reproduced below.

END

FILMED

7-85

DTIC